NASA Technical Memorandum 101383

Measured Far-Field Flight Noise of a Counterrotation Turboprop at Cruise Conditions

Richard P. Woodward, Irvin J. Loeffler,
and James H. Dittmar
Lewis Research Center
Cleveland, Ohio

January 1989

NASA

MEASURED FAR-FIELD FLIGHT NOISE OF A COUNTERROTATION TURBOPROP AT CRUISE CONDITIONS

Richard P. Woodward, Irvin J. Loeffler, and James H. Dittmar
National Aeronautics and Space Administration
Lewis Research Center
Cleveland, Ohio 44135

SUMMARY

Modern high-speed propeller (advanced turboprop) aircraft are expected to operate on 50 to 60 percent less fuel than the 1980 vintage turbofan fleet while at the same time matching the flight speed and performance of those aircraft. Counterrotation turboprop engines offer additional fuel savings by means of upstream propeller swirl recovery. This paper presents acoustic sideline results for a full-scale counterrotation turboprop engine at cruise conditions. The engine was installed on a Boeing 727 aircraft in place of the right-side turbofan engine. Acoustic data were taken from an instrumented Learjet chase plane. Sideline acoustic results are presented for 0.50 and 0.72 Mach cruise conditions. A scale model of the engine propeller was tested in a wind tunnel at 0.72 Mach cruise conditions. The model data were adjusted to flight acquisition conditions and were in general agreement with the flight results.

E-4437

INTRODUCTION

Modern high-speed propeller (advanced turboprop) aircraft are expected to operate on 50 to 60 percent less fuel than the 1980 vintage turbofan fleet while at the same time matching the flight speed and performance of those turbofan engines (ref. 1). Counterrotation propellers may offer from 8 to 10 percent of additional fuel savings over similar single-rotation propellers at cruise conditions. There is considerable concern, however, about the potential noise generated by such aircraft, including both in-flight cabin noise and community noise during takeoffs and landings. Enroute noise has only recently been raised as a potential concern. The data in this report provide a measure of source levels from which enroute projections can be made.

This report presents the acoustic test results for a full-scale counterrotation turboprop demonstrator engine installed on a Boeing 727 aircraft in place of the right-side turbofan engine (ref. 2) as shown in figure 1. Selected results from this study were also presented in reference 3. Sideline acoustic data were acquired from a Learjet chase plane that was instrumented with flush-mounted nose and wingtip microphones. Data are presented for a 47.2-m (155-ft) sideline at several engine operating conditions at 0.50 and 0.72 Mach numbers. Selected data are also compared with results from the test that was run in the NASA 8- by 6-Foot Wind Tunnel with a scale model of the counterrotation propeller.

APPARATUS AND PROCEDURE

This flight test was part of the General Electric Company's program to develop their unducted fan (UDF) counterrotation turboprop engine. The propeller has eight forward and eight aft blades. The forward propeller diameter is 3.57 m (11.7 ft), while the aft propeller diameter was reduced by 10 cm (4 in.) from this value for aeromechanical considerations.

Table I presents the flight test conditions for the tests discussed in this report. One test, designated flight condition 3.1, was flown at a 6523-m (21 400-ft) altitude and 0.50 Mach, and the remaining four tests were performed at a nominal 10 688-m (35 000-ft) altitude and 0.72 Mach. The propeller blade angles were automatically controlled in order to achieve an equal torque split between the two propellers. These propeller blade angles were nearly equal for the clean configuration wind tunnel tests and were also adjusted for an equal torque split. However, there was a considerable difference between the fore and aft blade angles, B_F and B_A, for the installed engine. This difference in blade-setting angles may be due to possible asymmetrical inflow to the UDF engine installed on the 727 aircraft.

Both the model and full-scale propeller power settings are expressed as total power density, PQAT, which is the power coefficient based on the annulus area of the forward rotor. PQAT is defined as

$$\frac{\text{Total power}}{(\rho)(\text{rev/sec})^3(D)^3(\text{annulus area})}$$

where ρ is the local air density and D is the forward rotor diameter. Reference 4 presents aerodynamic results for the model propeller.

Acoustic data were acquired with the NASA Lewis Learjet. Figure 2 is a photograph of the 727 aircraft in flight taken from the Learjet. The Learjet was instrumented with two nose and two wingtip microphones flush mounted on the left side of the aircraft. Acoustic and optical instrumentation described in reference 5 were also employed in the tests. The acoustic signals were monitored for data quality and recorded on magnetic tape aboard the aircraft for later analysis. The acoustic spectra of the Learjet engine noise were sufficiently different from those of the propeller to prevent significant data contamination. However, boundary-layer noise on the microphones generated an essentially flat broadband level of about 95 dB for a 3-Hz bandwidth over a 0- to 1200-Hz frequency range.

Figures 3 to 5 are photographs of the Learjet microphone installations. Figure 3 shows the wingtip region of the Learjet; figure 4 shows the location of the nose microphone. Figure 5 is a close view of the microphone mounting plate on the Learjet wingtip. Data presented in this paper are taken primarily at the wingtip microphone location. Directivity results for the nose microphone were often inconsistent with both the wingtip-measured directivities and with previously measured directivities for similar model turboprops tested acoustically in a wind tunnel environment.

Figure 6 is a sketch showing the sideline positioning of the two aircraft for sideline acoustic data acquisition. Data were taken for 60°, 90°, and 120° relative to the engine upstream axis for all flight conditions. Thirty-degree data were taken for two of the flight conditions; however, flying in

this position made it difficult to observe the 727 aircraft from the Learjet. The measured data were adjusted for spherical spreading to a nominal sideline distance of 47.2 m (155 ft) between the UDF engine axis and the Learjet wingtip. Most of the data points were actually taken close to this sideline separation.

Because of convective flow effects, the data angles presented in this paper are for "observed" angles to the turboprop rather than being corrected to "emission" angles. Figure 7 shows the relationship between the observed and emission angles. These differences can be significant. For example, the observed angles of 60°, 90°, and 120° at 0.72 Mach correspond, respectively, to emission angles of 21°, 44°, and 81°. At 0.50 Mach, these observed angles correspond to emission angles of 34°, 60°, and 94°.

Microphone sideline locations were determined by visual and photographic methods. A camera system mounted in the Learjet cabin was aimed at a target location on the 727 aircraft. The sideline angle was determined from a protractor device attached to the camera mount. The sideline distance was determined by image-size scaling of the in-flight photographs relative to similar photographs taken during static ground calibrations when the two aircraft were parked in the desired relative positions. The Learjet pilots used a simple optical comparator to establish roughly the sideline distance during flight. The acquired acoustic data were then adjusted for spherical divergence to a true 47.2-m (155-ft) sideline, which was the average separation distance. Table II presents the data acquisition positions for the five flight conditions, and shows the decibel corrections that were applied to the acoustic data for correction to the 47.2-m sideline. Table III lists the turboprop tone levels for each of the data positions.

RESULTS AND DISCUSSION

Sound Pressure Level Spectra

The sound pressure level (SPL) spectra for a counterrotation propeller are considerably more complex than those for a single-rotation propeller. The rotor-alone tones are present at each tone order (BPF, 2BPF, etc.). In addition, the higher-order tones (2BPF and above) contain rotor interaction tones. Figure 8 shows typical SPL spectra for the counterrotation propeller operating at equal fore and aft rotational speed. Since both rotors contain eight blades, the entire tone energy is concentrated in single spikes at multiples of the blade-passage frequency.

Most of the data were taken with a small difference in the two rotors' rotational speed (see table I). Figure 9 shows typical SPL spectra for this operating condition. The 1-Hz bandwidth allowed for a separation of the fore and aft rotor-alone tones. Also, the first interaction tone, BPF_F+BPF_A, is seen at 2BPF. Shaft-order tones are seen below the blade-passage frequency. One of the Learjet engine compressor tones appears just above 2BPF.

The SPL directivity results in this report were taken from spectra with 16- and 1-Hz bandwidths. The coarser 16-Hz bandwidth did not separate the components of the tone orders, even with the small rpm difference. The 1-Hz bandwidth allowed for tone separation at BPF and 2BPF with a nominal 40-rpm rotor

speed difference, thus providing a more detailed analysis of the tone generation mechanisms. Table III is a tabulation of these acoustic tone levels from the 16- and 1-Hz bandwidth spectra.

Sideline Directivities

Figure 10 shows the sideline directivities for the first four tone orders at 0.50 Mach (condition 3.1). Rotor-alone tones were not separated in this figure because of both the 16-Hz bandwidth and the essentially same fore and aft rotor rotational speed. They typically show a maximum level near the propeller plane, in contrast to the interaction tones that often have high levels away from this location. The rotor-alone fundamental (BPF) tones show the highest levels at all but the forward 26° location. The remaining tone orders (2 to 4BPF) in this figure contain interaction tones and do show relatively high levels at the forward angles. Sideline data at points approaching 30° were difficult to obtain because of awkward sighting angles from the Learjet and the difficulties of formation flight.

Figure 11 shows a comparison of the flyby and station-keeping directivities at 0.72 Mach (condition 5.1). Flyby data were only taken at condition 5.1. The flyby data were taken continuously as the Learjet slowly passed the 727 aircraft on a parallel course. The sideline angles for the flyby data are approximations based on angular reference points called out by Learjet pilots from hand-held sightings. These points were recorded on the data tape for later analysis. It was not possible to take camera reference photographs during the flyby. The flyby data were reduced at a 3-Hz bandwidth.

Flyby directivity traces are shown in figure 11 for both the wingtip and nose microphones. Corresponding data for the station-keeping points (table III, 16-Hz bandwidth) are also shown in this figure. As was previously mentioned, there was concern that the directivities measured by the nose microphone were not typical for turboprops. These data, therefore, are suspect. The results as shown for the wingtip and nose microphones are in fairly good agreement at sideline angles above 70°. At lower angles, however, the nose microphone results are significantly below those for the wingtip microphone. The BPF tone for the nose microphone at the 34° station-keeping position could not be separated in the acoustic spectra. This indicated that the tone level for the nose microphone was significantly below that for the wingtip microphone at this sideline angle.

The reason for this apparent discrepancy between the results for the wingtip and nose microphones is not immediately clear. The shape of the flyby directivities for both the nose and wingtip microphones in figure 11 suggests that there may be some reflections from the 727 aircraft and possibly from the Learjet structure as well. That is, the first-order rotor-alone tone directivity is expected to show a smooth peak without all the secondary undulations observed in the present flyby directivity. The relatively long wavelength of the acoustic signal (about 1.7 m (5.5 ft) at 299-Hz BPF) would tend to discount reflections from the Learjet structure. The location of the wingtip microphone on the Learjet is more favorable than that of the nose microphone because it is midway on a cylindrical surface with established boundary layers. Also, the wingtip is shielded from reflections by adjacent Learjet structure and is also closer to the noise source. In contrast, the nose microphones are located on an aircraft surface whose curvature is changing, but at a point

where the diameter is roughly equal to that of the wingtip tank. Boundary-layer refraction may also affect the data quality. Because of these concerns about the nose microphone data, the directivity results in this report will be presented for the wingtip microphone. However, the information in table III will allow the reader to construct directivities with the results from both microphones.

Figures 12 to 16 present the sideline directivities for the nominal 0.72 Mach flight tests. The two rotors were run at about a 40-rpm speed difference, making it possible to separate the tone components with 1-Hz bandwidth spectra. (Alternately, unequal rotor blade numbers would facilitate separation of the tone components.) Results are presented for each of the flight conditions for both 16-Hz bandwidth spectra with no tone-order separation, and for 1-Hz spectra that allowed for separation of the first- and second-order tone components.

Figure 12 shows the sideline directivities measured for condition 5.10, which had a PQAT value of 2.99 (table I). Figure 12(a) shows the directivities for the first four tone orders with no tone component separation (i.e., 16-Hz bandwidth analysis). The tone levels peak near 90°, while the forward rotor BPF tone increases toward the aft angles. The corresponding trend for the 2BPF forward rotor-alone tone is reversed, with the highest level at 59°. This result for the first-order rotor-alone tones contrasts with what has been generally observed for counterrotation turboprops. That is, the forward rotor-alone tone usually peaks upstream of the corresponding aft rotor-alone tone, with similar trends for higher-order rotor-alone tones.

The first interaction tone in figure 12(b) (1-Hz bandwidth analysis) is about 6 dB lower than the 2BPF aft rotor-alone tone. This is consistent with published model counterrotation turboprop results showing that, relative to rotor-alone tones, interaction tones are considerably higher at takeoff conditions than at cruise (refs. 6 and 7).

Figure 13 shows the directivities for condition 5.8, which had a PQAT value of 3.05. The directivities from the 16-Hz bandwidth spectra (fig. 13(a)) are quite similar to those of condition 5.10 (fig. 12(a)). However, the rotor-alone tone directivities at both BPF and 2BPF (fig. 13(b)) show that the forward rotor tends to have a peak rotor-alone tone somewhat aft of the aft rotor. These same data trends are evident for the condition 5.9 directivities (PQAT = 3.14) shown in figure 14. This tendency for the aft rotor-alone tone to peak upstream of the forward rotor-alone tone for the full-scale engine data contrasts with other published counterrotation propeller directivities. Model propeller results at cruise conditions (for example, see ref. 6) have always shown the forward rotor-alone tones to peak upstream of the corresponding aft rotor-alone tones. The reason for this discrepancy between the full-scale and model directivities is not known.

Figure 15 presents the sideline directivities for condition 5.1, which had a PQAT value of 4.24 with the aircraft at cruise conditions of 0.72 Mach at a 10 688-m (35 000-ft) altitude. The UDF engine was at a 100-percent power setting at this operating condition. The 16-Hz bandwidth (fig. 15(a)) again shows that the first-order rotor-alone tones dominate the directivity. The 1-Hz bandwidth directivities (fig. 15(b)), which allowed separation of the fore and aft rotor-alone tones, show both of these tones peaking near 90°.

Comparison With Wind Tunnel Results

A 62.2-cm (24.5-in.) diameter model of the engine propeller was acoustically tested earlier in the NASA Lewis 8- by 6-Foot Wind Tunnel (fig. 16). Figure 17 shows details of the model propeller installation in this wind tunnel. Sideline directivity data were acquired from microphones flush mounted on a flat plate that was lowered from the tunnel ceiling. Data for a test condition that approximated the 0.72-Mach engine conditions were selected for this comparison. The wind tunnel results were adjusted to "as measured" conditions equivalent to the flight data. These adjustments included corrections for pressure altitude, propeller size, and distance (ref. 8). The wind tunnel data were also adjusted (fig. 3) for expected noise increase above free field due to the presence of the Learjet tip tank wall in which the microphone was mounted (ref. 9). The correction for measurement on the approximately 0.6-m (2-ft) diameter Learjet wingtip tank was 5 dB above free field for the fundamental rotor-alone tone.

In figure 18, the wind tunnel acoustic fundamental tone level, adjusted to the aircraft flight conditions, is plotted against the observed sideline angle. Also shown are the corresponding flight test data for four UDF propeller operating conditions at a nominal 0.72 Mach. There is general agreement between the wind tunnel and full-scale engine results. There are, however, a number of differences in the propeller operating conditions that merit further discussion. The engine results are shown for PQAT values of 2.99, 3.05, 3.14, and 4.24; the model data are for a 4.21 PQAT value. Tone levels for the engine operating at PQAT = 4.24 (100 percent power) would be expected to be somewhat higher than those for lower engine power settings. However, as seen in figure 18, tone levels associated with full-power operation were actually lower than those at lower power settings. The reason for this unexpected result remains unknown.

As previously mentioned, the blade-setting angles of the full-scale and model propellers were adjusted for approximately equal torque split between the two blade rows. The equal torque condition for the model propeller corresponds to blade pitch angles of 58.5° and 55.7°, which have a smaller difference between the fore and aft rotor than did the flight angles (see table I). This difference in blade-setting angles in the installed propeller may be the result of installation effects on the engine propeller inflow. In particular, a significantly nonaxial inflow near the aircraft fuselage and the presence of the support pylon could result in localized loading of one blade row and corresponding unloading of the other blade row in that region. This might account for the observed difference in engine propeller blade-setting angles. Reference 4 presents model propeller results in which the pylon installation effects affected the blade row torque split.

CONCLUDING REMARKS

Sideline acoustic data were obtained at cruise flight conditions for a full-scale counterrotation propeller engine that was installed on a Boeing 727 aircraft. These data were obtained with the acoustically instrumented NASA Lewis Learjet, which was flown in formation along a sideline relative to the counterrotation engine on the 727 aircraft. A unique set of cruise condition, sideline noise data were obtained. The shape of the sideline directivities suggests that acoustic reflections, particularly from the 727 aircraft, may be

affecting the data. Installation effects were also evidenced by the UDF engine, which had a significant difference in the fore and aft blade-setting angles. These angles, which are adjusted for an equal torque split between the two blade rows, were about equal in uninstalled model propeller tests at cruise conditions. The full-scale engine fundamental tone levels were in good general agreement with scaled-model propeller data from a wind tunnel test at similar flight speeds. However, the individual rotor-alone tone directivities for the engine tended to show the aft rotor tone peaking upstream of the forward rotor tone at partial power settings. This result contrasted with a number of model propeller studies in which the forward rotor-alone tones peaked upstream of the aft tones.

REFERENCES

1. Whitlow, J.B. Jr.; and Sievers, G.K.: Fuel Savings Potential of the NASA Advanced Turboprop Program. NASA TM-83736, 1984.

2. Reid, C.: Overview of Flight Testing of GE Aircraft Engines' Un-Ducted Fan. AIAA Paper 88-3082, July 1988.

3. Woodward, R.P.; Loeffler, I.J.; and Dittmar, J.H.: Cruise Noise of an Advanced Counterrotation Turboprop Measured from an Adjacent Aircraft. Noise-Con '88, J.S. Bolton, ed., Noise Control Foundation, Poughkeepsie, NY, 1988, pp. 105-110.

4. Sullivan, T.J.: Aerodynamic Performance of a Scale-Model, Counter-Rotating Unducted Fan. Advanced Technology for Aero Gas Turbine Components, AGARD CP-421, 1987, pp. 22-1 to 22-16.

5. Balombin, J.R.; and Loeffler, I.J.: Farfield Inflight Measurements of High-Speed Turboprop Noise. AIAA Paper 83-0745, Apr. 1983. (NASA TM-83327).

6. Dittmar J.H.; and Stang, D.B.: Noise Reduction for Model Counterrotation Propeller at Cruise by Reducing Aft-Propeller Diameter. NASA TM-88936, 1987.

7. Woodward, R.P.: Noise of a Model High Speed Counterrotation Propeller at Simulated Takeoff/Approach Conditions (F7/A7). AIAA Paper 87-2657, Oct. 1987. (NASA TM-100206).

8. Dittmar, J.H.; and Stang, D.B.: Cruise Noise of the 2/9 Scale Model of the Large-Scale Advanced Propfan (LAP) Propeller, SR-7A. AIAA Paper 87-2717, Oct. 1987. (NASA TM-100175).

9. Wiener, F.M.: Sound Diffraction by Rigid Spheres and Circular Cylinders. J. Acoust. Soc. Am., vol. 19, no. 3, May 1947, pp. 444-451.

TABLE I. - FLIGHT-TEST CONDITIONS

[100-Percent power is maximum engine climb; total power density PQAT is for forward rotor plane; blade-setting angle B is measured at 3/4-radius location; F = fore; A = aft.]

Flight condition	Mach number	Altitude		Ambient temperature, K	Power setting, percent	PQAT	Engine pressure ratio	Propeller thrust		Blade-setting angle, deg		Advance ratio		Physical speed	
		m	ft					N	lb/ft	B_F	B_A	J_F	J_A	rpm_F	rpm_A
3.1	0.50	6 523	21 400	250	100	2.67	3.58	35 350	7947	49.8	43.2	1.99	2.05	1340	1340
5.10	.71	9 815	32 200	227	62	2.99	2.97	15 079	3390	59.0	53.3	3.00	3.19	1205	1165
5.8	.72	10 851	35 600	224	69	3.05	3.20	14 408	3239	59.2	52.8	2.91	3.10	1249	1208
5.9	.72	9 906	32 500	226	76	3.14	3.39	18 380	4132	59.3	52.9	2.84	3.02	1286	1246
5.1	.72	10 668	35 000	226	100	4.24	4.06	21 440	4820	61.6	54.0	2.86	3.03	1278	1238

TABLE II. - STATION-KEEPING POSITIONS

Flight condition	Mach number	Wingtip microphones		Nose microphones	
		Observed angle, deg	ΔdB for 47.2-m (155-ft) sideline distance	Observed angle, deg	ΔdB for 47.2-m (155-ft) sideline distance
3.1	0.50	117	0.3	108	1.2
		90	.5	82	1.4
		59	.5	56	1.3
		26	-2.4	27	-1.2
5.1	.72	118	-.5	108	.5
		90	.3	82	1.2
		61	-.3	57	.5
		34	1.6	34	2.3
5.10	.71	116	.5	107	1.3
		89	.8	82	1.6
		60	.2	57	1.1
5.9	.72	114	-1.8	103	-.7
		88	.9	81	1.7
		60	1.5	57	2.3
5.8	.72	115	-.4	105	.6
		87	.5	80	1.4
		60	1.3	57	2.3

TABLE III. - ACOUSTIC DATA TABULATION

[Adjusted to 47.2-m (155-ft) sideline distance; BPF = tone order; F = fore; A = aft.]

Flight condition	Microphone location	Observed angle, deg	16-Hz bandwidth				1-Hz bandwidth				
			BPF	2BPF	3BPF	4BPF	BPF_F	BPF_A	$2BPF_F$	$2BPF_A$	BPF_F+BPF_A
			Noise, dB								
3.1	Nose	108	121	112.5	107	106	(a)	(a)	(a)	(a)	(a)
	↓	82	121.5	115	110	106.5	↓	↓	↓	↓	↓
		56	112	-----	-----	-----					
		27	-----	106	-----	-----					
	Wingtip	117	121	105	106	105					
	↓	90	121	111	112	105.5					
		59	119	107	103.5	105.5					
		26	100.5	110	103.5	102					
5.10	Nose	107	116	111.5	108.5	105	111	112	105	108	-----
		82	120.5	113.5	110	107	115.5	116.5	107	106	107.5
		57	109.5	107	-----	-----	103.5	103.5	-----	100.5	97
	Wingtip	116	118.5	107	-----	-----	120	106	100	102.5	-----
		89	122.5	114	111	108	116	122	101.5	111	105.5
		60	117	109	106.5	-----	115	113	104	105.5	100.5
5.8	Nose	105	122	115.5	112	105.5	118.5	119.5	111	112.5	107.5
		80	117	110	107.5	-----	102.5	114.5	-----	107.5	99.5
		57	110	107	105	-----	107	103.5	98.5	97	98
	Wingtip	115	119	110.5	105	106.5	120.5	113	111.5	107	-----
		87	124.5	116	112	109	121.5	124	110.5	111.5	113.5
		60	116.5	109	106	-----	114	114	102	103	-----
5.9	Nose	103	124	121	113	110	118.5	123.5	117.5	113.5	109.5
		81	117.5	112	110	106	110	118.5	102	109	100
		57	112	-----	-----	-----	106	106.5	-----	99	100
	Wingtip	114	123	117	112.5	108	123	115.5	114	108	99
		88	123.5	118.5	112	108.5	120	125	107	115.5	115
		60	114	108	-----	-----	112	112	99.5	102	102
5.1	Nose	108	124.5	113.5	108	108	123	121	110.5	106	111.5
	↓	82	113	112	109	105	111	112	97	110	99
		57	109	105	-----	-----	-----	-----	-----	-----	-----
		34	-----	-----	-----	-----	-----	-----	-----	-----	-----
	Wingtip	118	116.5	108	110	109.5	113	117	104	109	97
	↓	90	120.5	115	114.5	107.5	117	121	111	112	101
		61	116	109	106	-----	113.5	114	98	105	103.5
		34	109	-----	-----	-----	104	107.5	96.5	99	97

[a]Insufficient rotor-speed difference to separate tones for this condition.

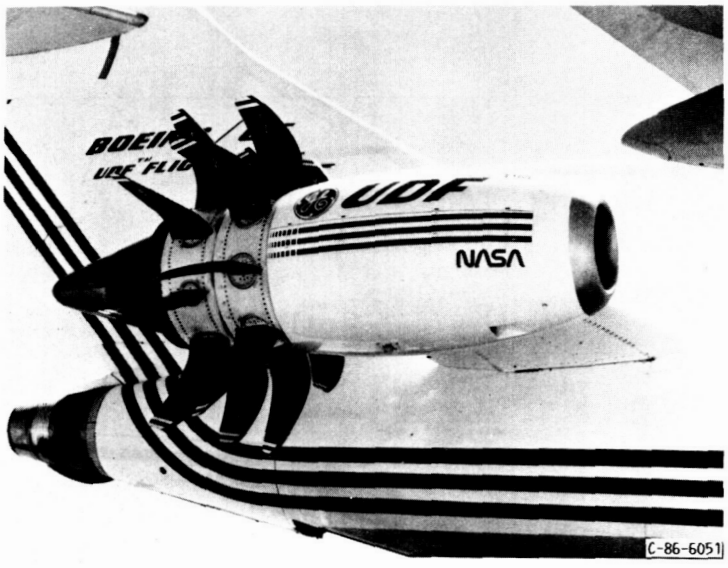

FIGURE 1. - PHOTOGRAPH OF COUNTERROTATION TURBOPROP ENGINE INSTALLED ON BOEING 727 AIRCRAFT.

FIGURE 2. - PHOTOGRAPH OF BOEING 727 AIRCRAFT WITH UDF ENGINE, TAKEN FROM LEARJET WHOSE WINGTIP IS IN FOREGROUND.

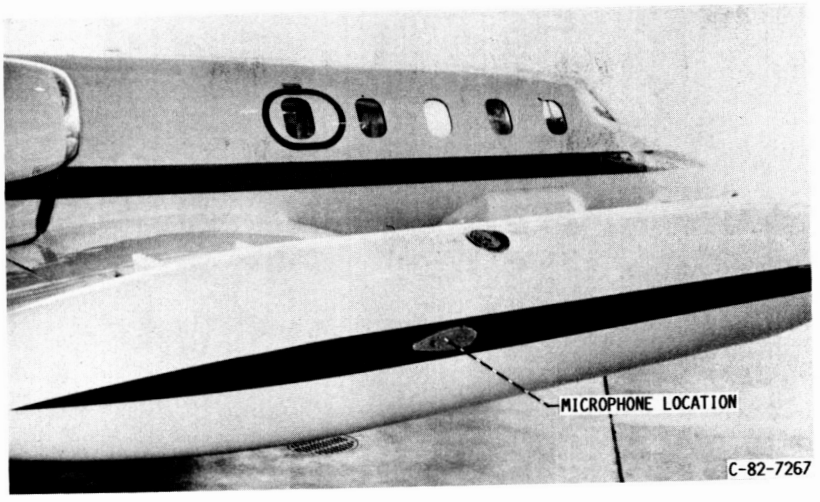

FIGURE 3. - LEARJET WINGTIP MICROPHONE INSTALLATION.

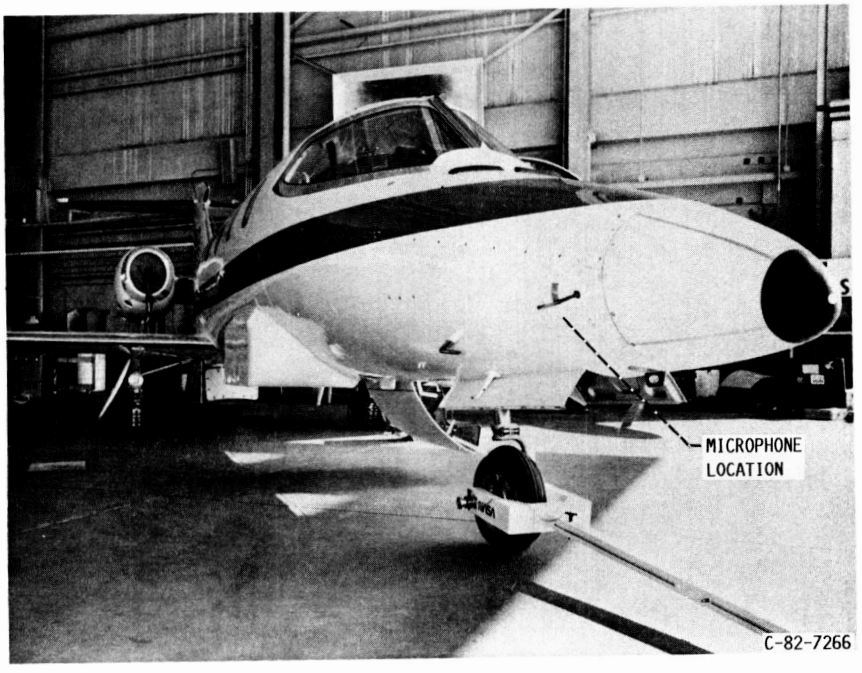

FIGURE 4. - LEARJET NOSE MICROPHONE INSTALLATION.

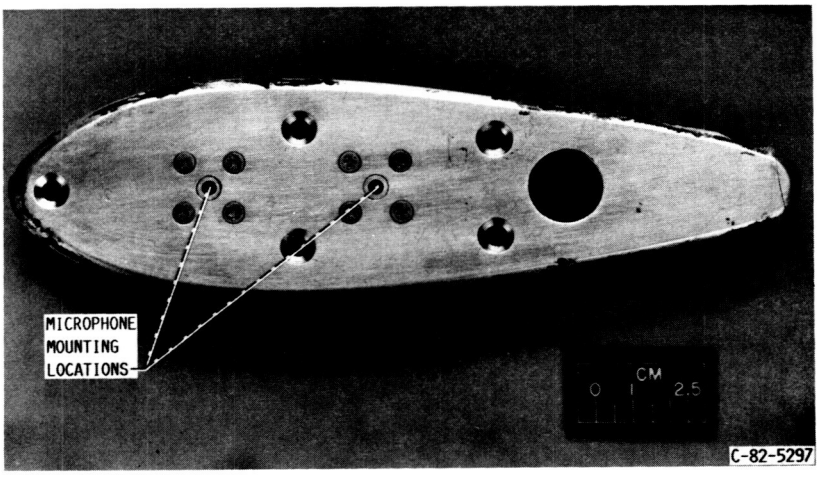

FIGURE 5. - WINGTIP MICROPHONE MOUNTING PLATE.

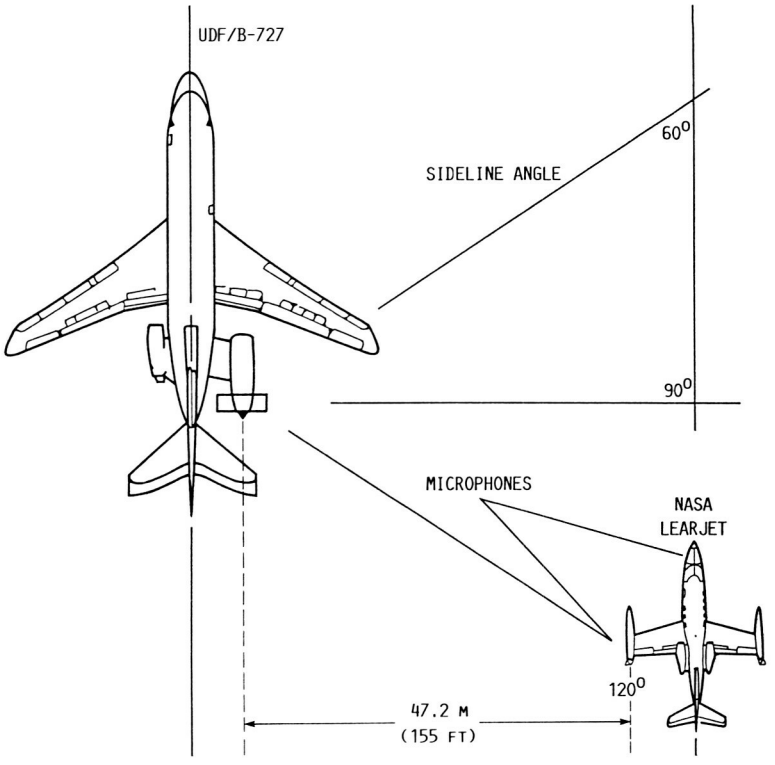

FIGURE 6. - SCHEMATIC OF LEARJET SIDELINE POSITIONING FOR ACOUSTIC DATA ACQUISITION.

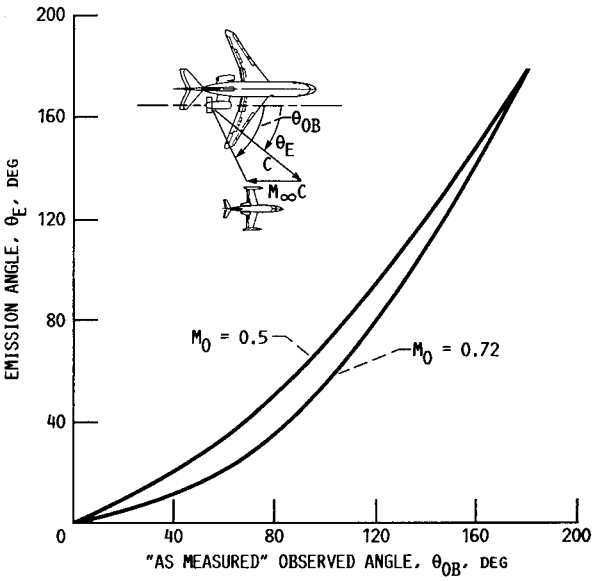

FIGURE 7. - RELATIONSHIP BETWEEN OBSERVED AND EMISSION ANGLES. $\theta_E = \theta_{OB} - \sin^{-1}(M_0 \sin \theta_{OB})$.

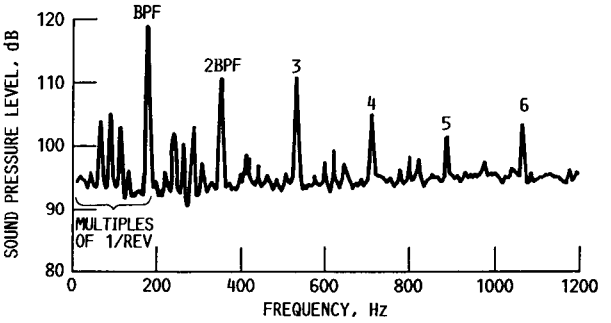

FIGURE 8. - TYPICAL SOUND PRESSURE LEVEL SPECTRA. ALTITUDE, 6523 M (21 400 FT); 0.50 MACH. CONDITION 3.1; TOTAL POWER DENSITY, 2.67; BLADE-SETTING ANGLES: FORE, 49.8°; AFT, 43.2°; SIDELINE ANGLE, 90°; LEARJET WINGTIP MICROPHONE; BANDWIDTH, 3 Hz. PROPELLER OPERATION AT EQUAL FORE AND AFT ROTATIONAL SPEED. BPF = TONE ORDER.

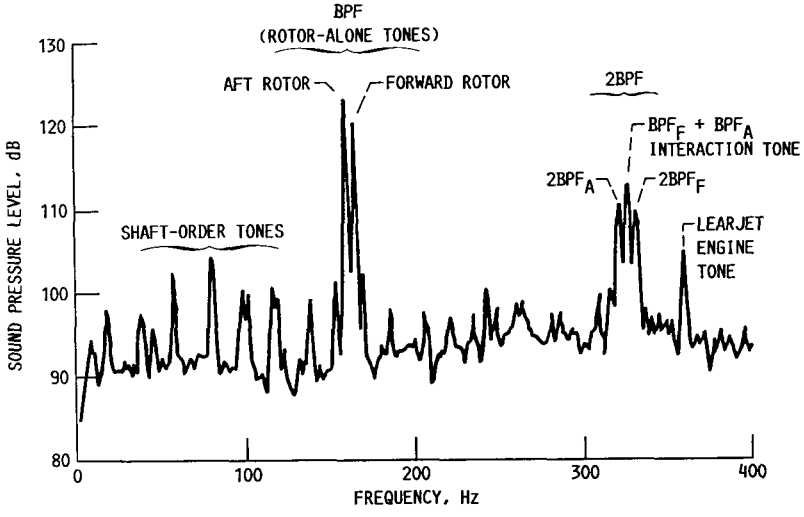

FIGURE 9. - TYPICAL SOUND PRESSURE LEVEL SPECTRA. ALTITUDE, 10 851 M (35 600 FT); 0.72 MACH; TOTAL POWER DENSITY, 3.05; BLADE-SETTING ANGLES: FORE, 59.2°; AFT, 52.8°; SIDELINE ANGLE, 87°; LEARJET WINGTIP MICROPHONE; BANDWIDTH, 1.0 Hz. BPF = TONE ORDER; F = FORE; A = AFT.

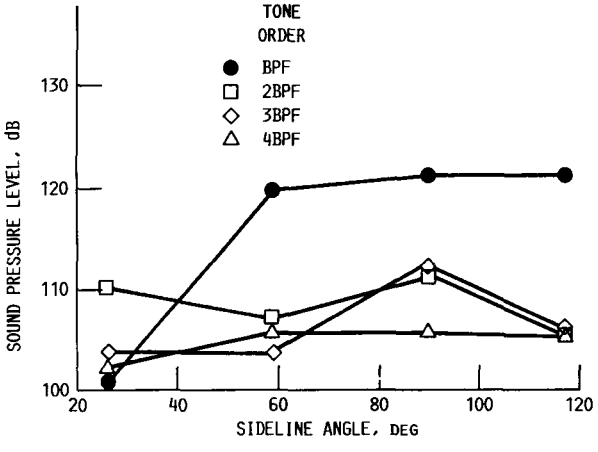

FIGURE 10. - SIDELINE SOUND PRESSURE LEVEL DIRECTIVITY FOR UDF ENGINE AT 0.50 MACH. CONDITION 3.1; ALTITUDE, 6523 M (21 400 FT); TOTAL POWER DENSITY, 2.67; BLADE-SETTING ANGLES: FORE, 49.8°; AFT, 43.2°; SIDELINE DISTANCE, 47.2 M (155 FT); BANDWIDTH, 16 Hz. BPF = TONE ORDER.

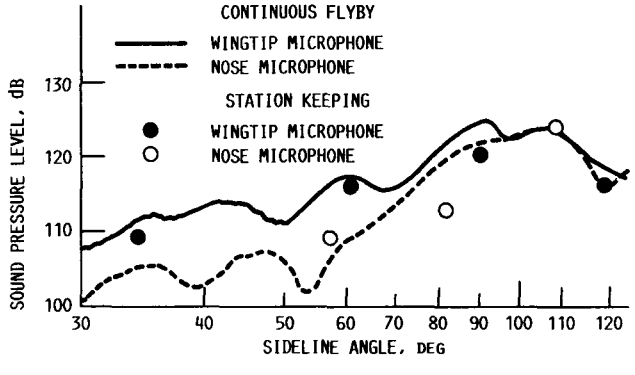

FIGURE 11. - SIDELINE SOUND PRESSURE LEVEL DIRECTIVITY FOR UDF ENGINE AT 0.72 MACH. CONDITION 5.1; SIDELINE DISTANCE, 47.2 M (155 FT).

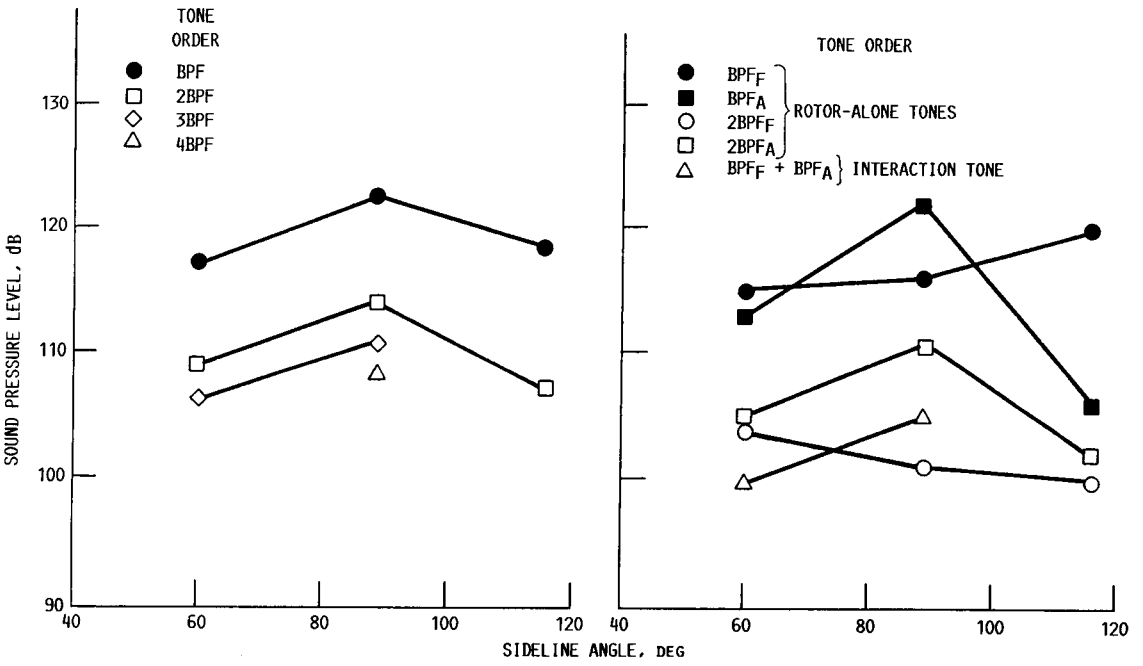

(A) 16-Hz BANDWIDTH. (B) 1-Hz BANDWIDTH.

FIGURE 12. - SIDELINE SOUND PRESSURE LEVEL DIRECTIVITY FOR UDF ENGINE AT 0.72 MACH. CONDITION 5.1; ALTITUDE, 9815 M (32 200 FT); TOTAL POWER DENSITY, 2.99; BLADE-SETTING ANGLES: FORE, 59.0°; AFT, 53.3°; SIDELINE DISTANCE, 47.2 M (155 FT). BPF = TONE ORDER; F = FORE; A = AFT.

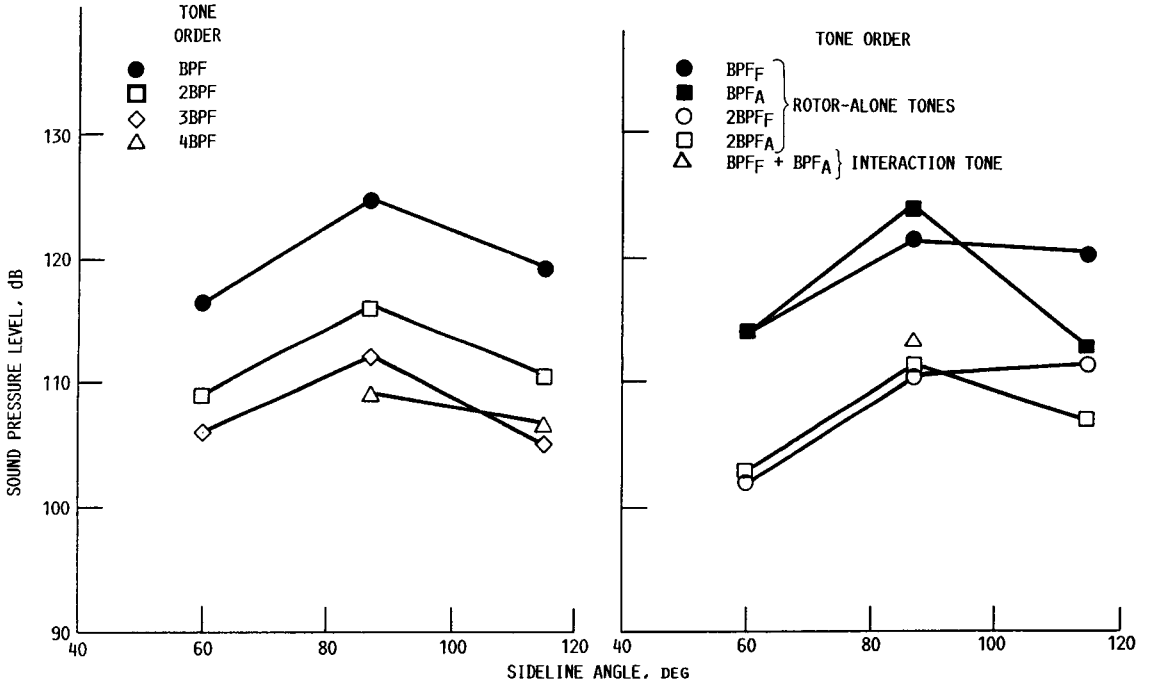

(A) 16-Hz BANDWIDTH. (B) 1-Hz BANDWIDTH.

FIGURE 13. - SIDELINE SOUND PRESSURE LEVEL DIRECTIVITY FOR UDF ENGINE AT 0.72 MACH. CONDITION 5.8; ALTITUDE, 10 851 M (35 600 FT); TOTAL POWER DENSITY, 3.05; BLADE-SETTING ANGLES: FORE, 59.2°; AFT, 52.8°; SIDELINE DISTANCE, 47.2 M (155 FT). BPF = TONE ORDER; F = FORE; A = AFT.

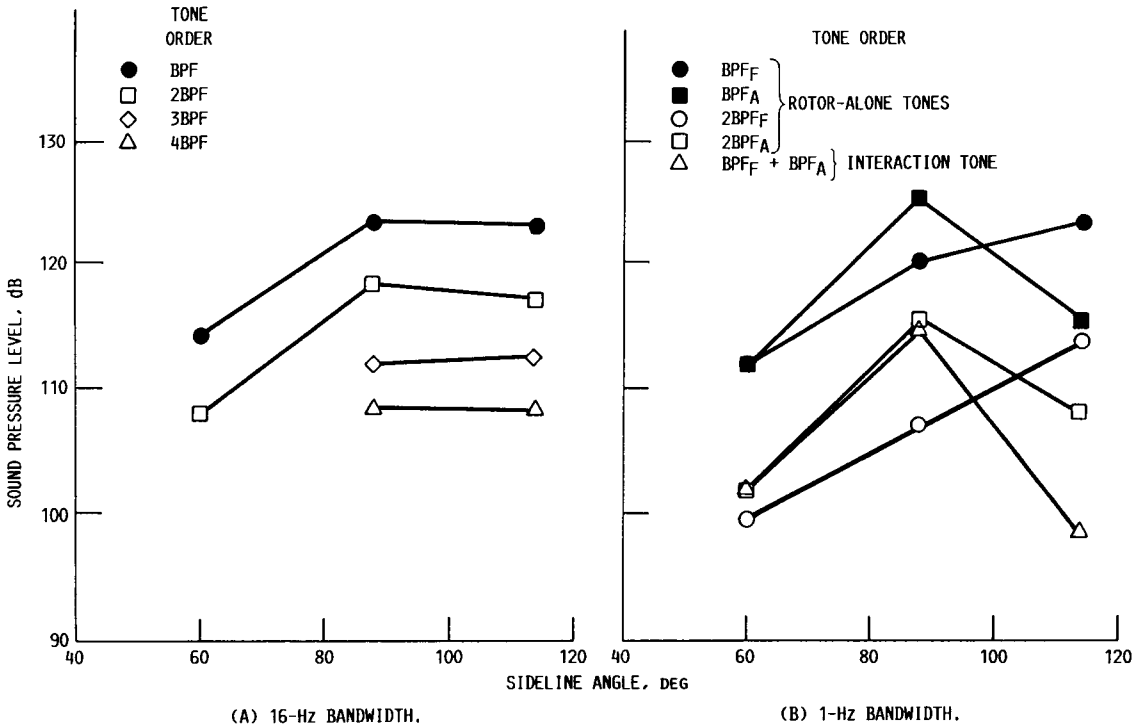

FIGURE 14. - SIDELINE SOUND PRESSURE LEVEL DIRECTIVITY FOR UDF ENGINE AT 0.72 MACH. CONDITION 5.9; ALTITUDE, 9906 M (32 500 FT); TOTAL POWER DENSITY, 3.14; BLADE-SETTING ANGLES: FORE, 59.3°; AFT, 52.9°; SIDELINE DISTANCE, 47.2 M (155 FT). BPF = TONE ORDER; F = FORE; A = AFT.

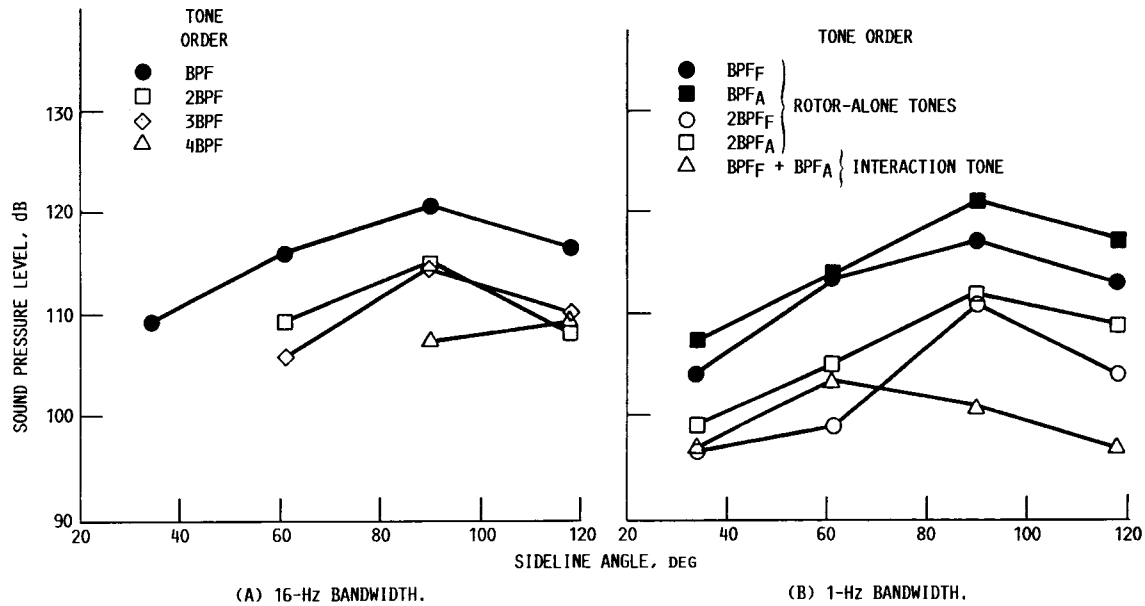

FIGURE 15. - SIDELINE SOUND PRESSURE LEVEL DIRECTIVITY FOR UDF ENGINE AT 0.72 MACH. CONDITION 5.1; ALTITUDE, 10 688 M (35 000 FT); TOTAL POWER DENSITY, 4.24; BLADE-SETTING ANGLES: FORE, 61.6°; AFT, 54.0°; SIDELINE DISTANCE, 47.2 M (155 FT). BPF = TONE ORDER; F = FORE; A = AFT.

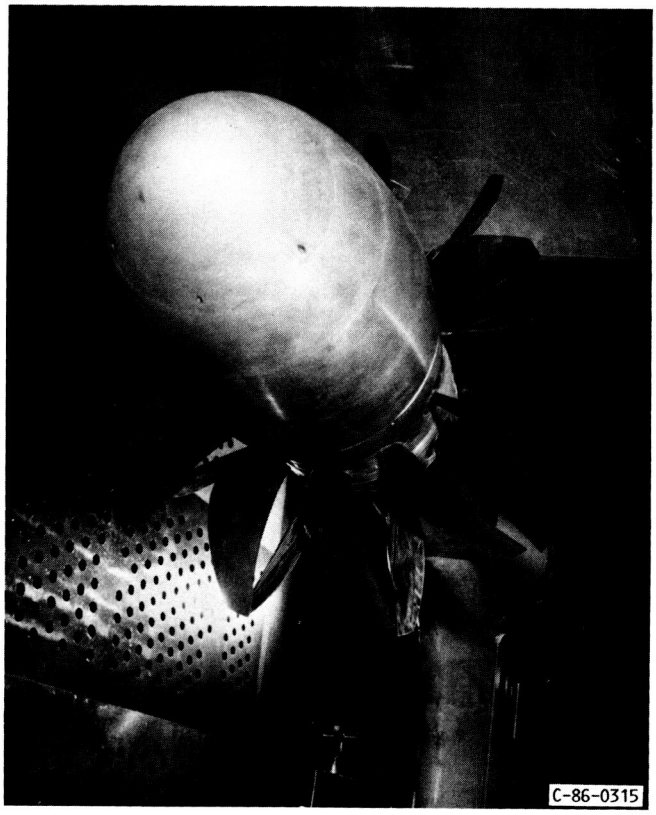

FIGURE 16. - MODEL PROPELLER TESTED IN NASA LEWIS 8- BY 6-FOOT WIND TUNNEL.

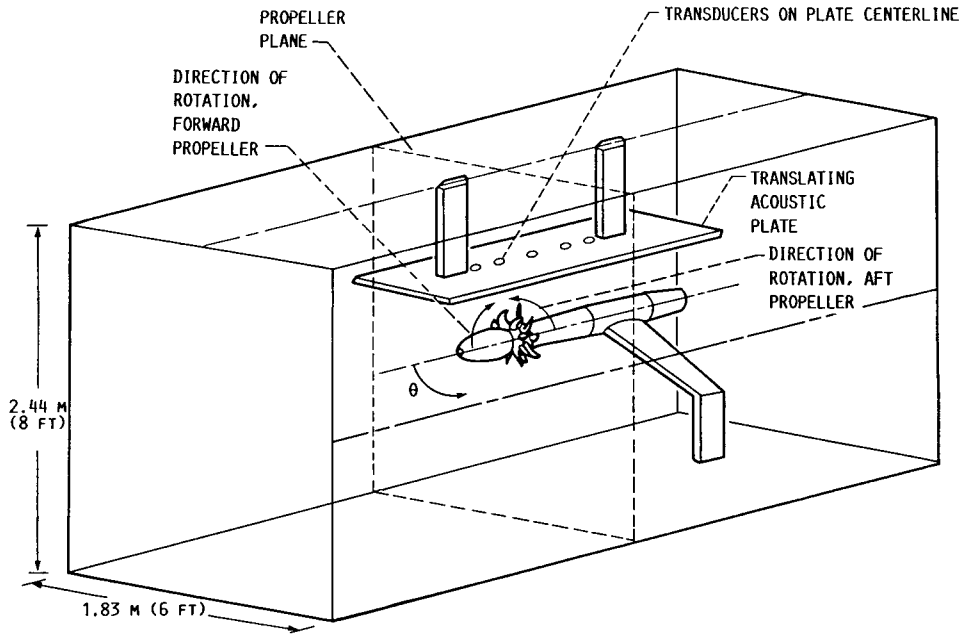

FIGURE 17. - TEST APPARATUS SHOWING TRANSLATING ACOUSTIC PLATE.

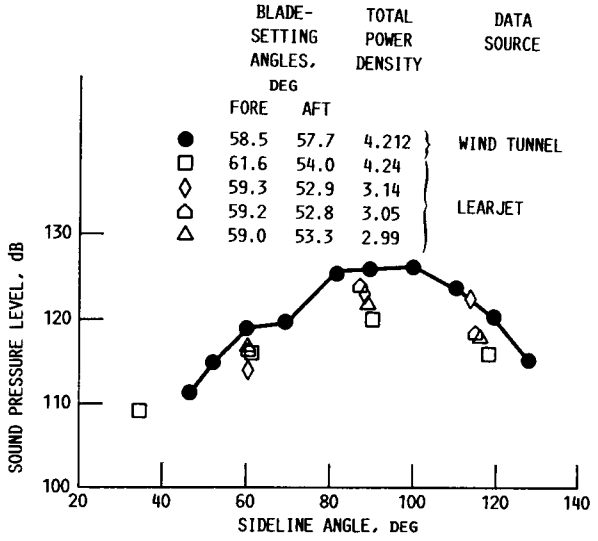

FIGURE 18. - COMPARISON OF SIDELINE TONE ORDER DIRECTIVITIES FOR UDF ENGINE AND MODEL PROPELLER. MODEL DATA SCALED TO FLIGHT CONDITIONS. 0.72 MACH; SIDELINE DISTANCE, 47.2 M (155 FT); NOMINAL ALTITUDE, 10 688 M (35 000 FT); LEARJET WINGTIP MICROPHONE.

NASA
National Aeronautics and Space Administration

Report Documentation Page

1. Report No.	2. Government Accession No.	3. Recipient's Catalog No.
NASA TM-101383		

4. Title and Subtitle	5. Report Date
Measured Far-Field Flight Noise of a Counterrotation Turboprop at Cruise Conditions	January 1989
	6. Performing Organization Code

7. Author(s)	8. Performing Organization Report No.
Richard P. Woodward, Irvin J. Loeffler, and James H. Dittmar	E-4437
	10. Work Unit No. 535-03-01

9. Performing Organization Name and Address	11. Contract or Grant No.
National Aeronautics and Space Administration Lewis Research Center Cleveland, Ohio 44135-3191	
	13. Type of Report and Period Covered Technical Memorandum

12. Sponsoring Agency Name and Address	14. Sponsoring Agency Code
National Aeronautics and Space Administration Washington, D.C. 20546-0001	

15. Supplementary Notes

16. Abstract

Modern high-speed propeller (advanced turboprop) aircraft are expected to operate on 50 to 60 percent less fuel than the 1980 vintage turbofan fleet while at the same time matching the flight speed and performance of those aircraft. Counterrotation turboprop engines offer additional fuel savings by means of upstream propeller swirl recovery. This paper presents acoustic sideline results for a full-scale counterrotation turboprop engine at cruise conditions. The engine was installed on a Boeing 727 aircraft in place of the right-side turbofan engine. Acoustic data were taken from an instrumented Learjet chase plane. Sideline acoustic results are presented for 0.50 and 0.72 Mach cruise conditions. A scale model of the engine propeller was tested in a wind tunnel at 0.72 Mach cruise conditions. The model data were adjusted to flight acquisition conditions and were in general agreement with the flight results.

17. Key Words (Suggested by Author(s))	18. Distribution Statement
Noise Flight Counterrotation Turboprop	Unclassified – Unlimited Subject Category 71

19. Security Classif. (of this report)	20. Security Classif. (of this page)	21. No of pages	22. Price*
Unclassified	Unclassified	20	A03

*For sale by the National Technical Information Service, Springfield, Virginia 22161